Carbohydrate Research, 208 (1990) 117–126
Elsevier Science Publishers B.V., Amsterdam

ROESY studies and HSEA calculations on xylose-containing oligosaccharides related to *N*-glycoproteins

Bas R. Leeflang, Jan B. Bouwstra, Janos Kerékgyártó*, Johannis P. Kamerling, and Johannes F. G. Vliegenthart

Department of Bio-Organic Chemistry, Transitorium III, Utrecht University, P.O. Box 80.075, NL-3508 TB Utrecht (The Netherlands)

(Received January 30th, 1990; accepted for publication, April 23rd, 1990)

ABSTRACT

Conformational studies on β-D-Xyl-(1→2)-[α-D-Man-(1→6)]-β-D-Man-OMe, β-D-Xyl-(1→2)-[α-D-Man-(1→3)]-β-D-Man-OMe, and β-D-Xyl-(1→2)-[α-D-Man-(1→3)]-[α-D-Man-(1→6)]-β-D-Man-OMe have been carried out using rotating-frame n.O.e. experiments in combination with HSEA calculations. The estimated time-averaged torsional angles Φ and Ψ about the various glycosidic linkages and the estimated time-averaged rotamer population around the C-5–C-6-linkage of β-Man in the tetrasaccharide are similar to the corresponding parameters for both trisaccharides.

INTRODUCTION

As part of our studies of xylose-containing *N*-linked carbohydrate chains[1–9], β-D-Xyl-(1→2)-[α-D-Man-(1→6)]-β-D-Man-OMe (**1**), β-D-Xyl-(1→2)-[α-D-Man-(1→3)]-β-D-Man-OMe (**2**), and β-D-Xyl-(1→2)-[α-D-Man-(1→3)]-[α-D-Man-(1→6)]-β-D-Man-OMe (**3**), representing structural elements of naturally occurring oligosaccharides, have been synthesised[7] and characterised by n.m.r. spectroscopy[8]. We now present conformational data for **1–3** obtained by rotating-frame n.O.e. (ROESY) experiments[10–15] in combination with HSEA calculations[16–19].

EXPERIMENTAL

N.m.r. methods. — N.m.r. spectra of 15mM solutions of the oligosaccharides **1**, **2**, and **3** were recorded at 27°. Prior to n.m.r. spectroscopy, the samples were repeatedly exchanged in 99.75% D_2O with intermediate lyophilisation, finally using 99.96% D_2O (Aldrich). In order to enhance the sensitivity in the ^1H–^1H ROESY[10–15] experiments, the samples were degassed in the n.m.r. tube by repeated evacuation, and sealed under argon. The experiments were carried out with a Bruker AM-500 spectrometer (Department of NMR Spectroscopy, Utrecht University; SON hf-NMR facility, Department of Biophysical Chemistry, Nijmegen University), equipped with an Aspect-3000 computer, using the sequence 90°–t_1–SL–acq(t_2), wherein SL is a single 200-ms spin-lock

* On leave from the Institute of Biochemistry, L. Kossuth University, Debrecen, Hungary.

0008-6215/90/$ 03.50

pulse (field strength, 2500 Hz). An 8-pulse phase program was applied[12], which included a 180° phase alternation for the spin-lock pulse between consecutive scans. A 90° phase difference between the 90° pulse and the spin-lock pulse was kept at all times. The spectral width was 3333.33 Hz in both dimensions and 520 t_1 increments were used for one experiment. Spectra were measured in the phase-sensitive mode, using quadrature detection in F2 and time-proportional phase increments (TPPI)[20]. A 520 × 2k data matrix was acquired, which was zero filled and multiplied with a $\pi/2$ phase shifted sine-bell prior to a phase-sensitive F.t. in order to obtain a 1k × 1k data matrix. Chemical shifts (δ) are expressed in p.p.m. downfield from internal sodium 4,4-dimethyl-4-silapentane-1-sulphonate (DSS), but were actually measured by reference to internal acetone (δ 2.225). The spectral offset (O_1) used for compounds **1**, **2**, and **3** was at δ 5.9, 6.3, and 5.6, respectively, thereby minimising the Hartmann–Hahn transfer.

Distance constraints. — Cross-peak intensities were corrected for their offset from the carrier frequency by a correction factor[14]:

$$1 / (\sin^2\theta_i \cdot \sin\theta_j),$$
$$\text{with } \tan(\theta_{i,j}) = \gamma_{i,j}B_{s1} / (\omega_{i,j} - \omega_0),$$

where γB_{s1} is the strength of the spin-lock field in Hz. The peak was detected at the frequency of proton i with a modulation of the frequency of proton j.

Each inter-residue ^1H–^1H distance was calculated from the two rotating-frame n.O.e. cross-peaks between the two resonances by relating their intensities to eight intensities of four ^1H–^1H pairs at known distances from each other (1.78–2.56 Å[21]) by the equation $r_{ij} = r_0(a_0/a_{ij})^{1/6}$ (r_{ij}, distance to be determined; r_0, known distance; a_{ij}, cross-peak intensity of a pair of protons at an unknown distance; a_0, cross-peak intensity of a pair of protons at a known distance)[22]. The 16 resulting values were averaged, giving the distance and the estimated error. The same method was applied to the intra-residue ^1H–^1H pairs that were taken as references, in order to check the internal consistency.

Energy calculations. — The HSEA program[16–19], taking into account non-bonded interactions as expressed by the Kitaigorodsky algorithm, together with a term for the exo-anomeric effect, was used to estimate the preferred conformations for each glycosidic linkage. In the Φ/Ψ domain, iso-energy contour levels were calculated with steps of 0.5 kcal/mol. The torsional angle Φ is defined as (O-5′,C-1′,O-x,C-x) with $x = 2, 3, 4$, or 6; the torsional angle Ψ as (C-1′,O-x, C-x, C-{x-1}) with $x = 2, 3, 4$, or 6; the bond angle τ (C-1′,O-x,C-x) is set at 117°. The dihedral angle ω is defined as (O-6,C-6,C-5,C-4)*.

Molecular modelling. — Molecular modelling has been carried out on an Evans & Sutherland PS300 graphic display work-station, and geometry calculations were performed on a local VAX cluster by use of the software program Platon[23].

* In this study, the IUPAC rules for defining torsional angles in carbohydrates have been used.

RESULTS AND DISCUSSION

In order to obtain conformational data for **1**, **2**, and **3** by n.m.r. spectroscopy, inter-residue ^1H–^1H distances are calculated by comparing the corresponding cross-relaxation rates with those of intra-residue ^1H–^1H pairs at known distances from each other. ^1H–^1H ROESY instead of ^1H–^1H NOESY experiments are used, because, in the latter at 500 MHz, the correlation time τ_c approaches the inverse of the Larmor frequency, resulting in near-to-zero cross-peak intensities, whereas, in rotating-frame experiments, the effective Larmor frequency is low, as compared to the molecular reorientation rates[10]. However, under conditions used for ^1H–^1H ROESY experiments, Homonuclear Hartmann Hahn (HOHAHA) type of magnetisation transfer might occur[13], thereby hampering the interpretation of ROESY effects in terms of ^1H–^1H distances. In order to suppress these interfering effects, the experimental conditions have to be chosen carefully[14]. It is known that the rate of the HOHAHA type of coherent magnetisation transfer between two protons is slowed down by a large absolute difference of their respective offsets[12], by a minimal spin-lock field strength, and by a small coupling constant between them. Therefore, the offset was positioned at the far low side of the spectrum and the spin-lock field strength was minimised so that, for protons at the high-field side of the spectrum, θ was $\sim 60°$ (ref. 14). The cross-peak intensities were corrected for the decrease in spin-lock efficiency at increasing offset from the carrier frequency. The intensities were not normalised, because overlap on the diagonal prohibited accurate measurement of diagonal intensities. However, this is not a serious problem, because only intensities within the same experiment have to be correlated. Cross-peaks arising from intra-residue ^1H–^1H pairs at known distances can be used as references to determine other ^1H–^1H distances from their cross-peaks. In Table I, reference[21] and calculated ^1H–^1H distances together with the estimated errors are given. For each compound, four intra-residue ^1H–^1H pairs with distances ranging from 1.78 to 2.56 Å were taken as references. With two cross-peaks per ^1H–^1H pair, sixteen different values for the distance are obtained. Simple statistics give the averaged distance and its standard deviation as its estimated error. As a typical example, the ^1H–^1H ROESY spectrum of **3** is depicted in Fig. 1.

HSEA calculations carried out on the complete oligosaccharides were used to determine the iso-energy contours for the glycosidic linkages. The iso-energy contour maps of **3** are shown in Fig. 2. Each structure is discussed separately.

β-D-*Xyl-(1→2)-[α*-D-*Man-(1→6)]-β*-D-*Man-OMe* (**1**). — For the α-Man-(1→6)-Man linkage, the rotamer population in Man-*3* (for explanation of the code system, see Table I) is calculated[24] from the vicinal coupling constants[8] $J_{5,6}$ (2.3 Hz) and $J_{5,6'}$ (5.2 Hz), yielding a rotamer population of $P_{\omega=60}$:$P_{\omega=180}$:$P_{\omega=-60}$ = 40:60:0 (Table II). Analysis of the cross-relaxation data between H-1 of Man-*4'* and H-6,6' of Man-*3* shows the H-1–H-6 and H-1–H-6' distances to be 3.0 and 2.4 Å, respectively (Table I). Each distance constraint can be realised by a range of Φ/Ψ values. Based on the combination of both Φ/Ψ ranges, the conformation about the α-(1→6) linkage is described by Φ/Ψ 70/180 (Table II). For the *β*-Xyl-(1→2)-Man linkage, the interglycosidic ROESY effect

TABLE I

Cross-peak intensities, intra-residue distances, and calculated inter-residue distances between the protons of the constituent monomers of **1**, **2**, and **3** (*β*-Man ≡ Man-*3*, α-Man-(1→6) ≡ Man-*4'*, α-Man-(1→3) ≡ Man-*4*)

β-D-*Xyl-(1→2)-[α*-D-*Man-(1→6)]-β*-D-*Man-OMe* (**1**)

	^1H–^1H connectivity				*Reference distance* (Å)	*Calculated distance* (Å)	*Estimated error* (Å)
Intra-residue	H-1	Xyl	H-5*a*	Xyl	2.50	2.4	0.1
	H-5*a*	Xyl	H-5*e*	Xyl	1.78	1.9	0.1
	H-1	Man-*3*	H-2	Man-*3*	2.45	2.4	0.1
	H-1	Man-*4'*	H-2	Man-*4'*	2.56	2.6	0.1
Inter-residue	H-1	Xyl	H-2	Man-*3*		2.3	0.1
	H-1	Man-*4'*	H-6	Man-*3*		3.0	0.15
	H-1	Man-*4'*	H-6'	Man-*3*		2.4	0.1

β-D-*Xyl-(1→2)-[α*-D-*Man-(1→3)]-β*-D-*Man-OMe* (**2**)

	^1H–^1H connectivity				*Reference distance* (Å)	*Calculated distance* (Å)	*Estimated error* (Å)
Intra-residue	H-1	Xyl	H-5*a*	Xyl	2.50	2.4	0.1
	H-5*a*	Xyl	H-5*e*	Xyl	1.78	1.9	0.1
	H-1	Man-*3*	H-2	Man-*3*	2.45	2.4	0.1
	H-1	Man-*4*	H-2	Man-*4*	2.56	2.5	0.1
Inter-residue	H-1	Xyl	H-2	Man-*3*		2.2	0.1
	H-3	Man-*3*	H-1	Man-*4*		2.25	0.1
	H-2	Man-*3*	H-5	Man-*4*		2.4	0.1

β-D-*Xyl-(1→2)-[α*-D-*Man-(1→3)]-[α*-D-*Man-(1→6)]-β*-D-*Man-OMe* (**3**)

	^1H–^1H connectivity				*Reference distance* (Å)	*Calculated distance* (Å)	*Estimated error* (Å)
Intra-residue	H-5*a*	Xyl	H-5*e*	Xyl	1.78	1.9	0.1
	H-1	Man-*3*	H-2	Man-*3*	2.45	2.4	0.1
	H-1	Man-*4*	H-2	Man-*4*	2.56	2.6	0.1
	H-1	Man-*4'*	H-2	Man-*4'*	2.56	2.6	0.1
Inter-residue	H-1	Xyl	H-2	Man-*3*		2.2	0.1
	H-3	Man-*3*	H-1	Man-*4*		2.3	0.1
	H-2	Man-*3*	H-5	Man-*4*		2.4	0.2
	H-1	Man-*4'*	H-6	Man-*3*		3.2	0.15
	H-1	Man-*4'*	H-6'	Man-*3*		2.4	0.1

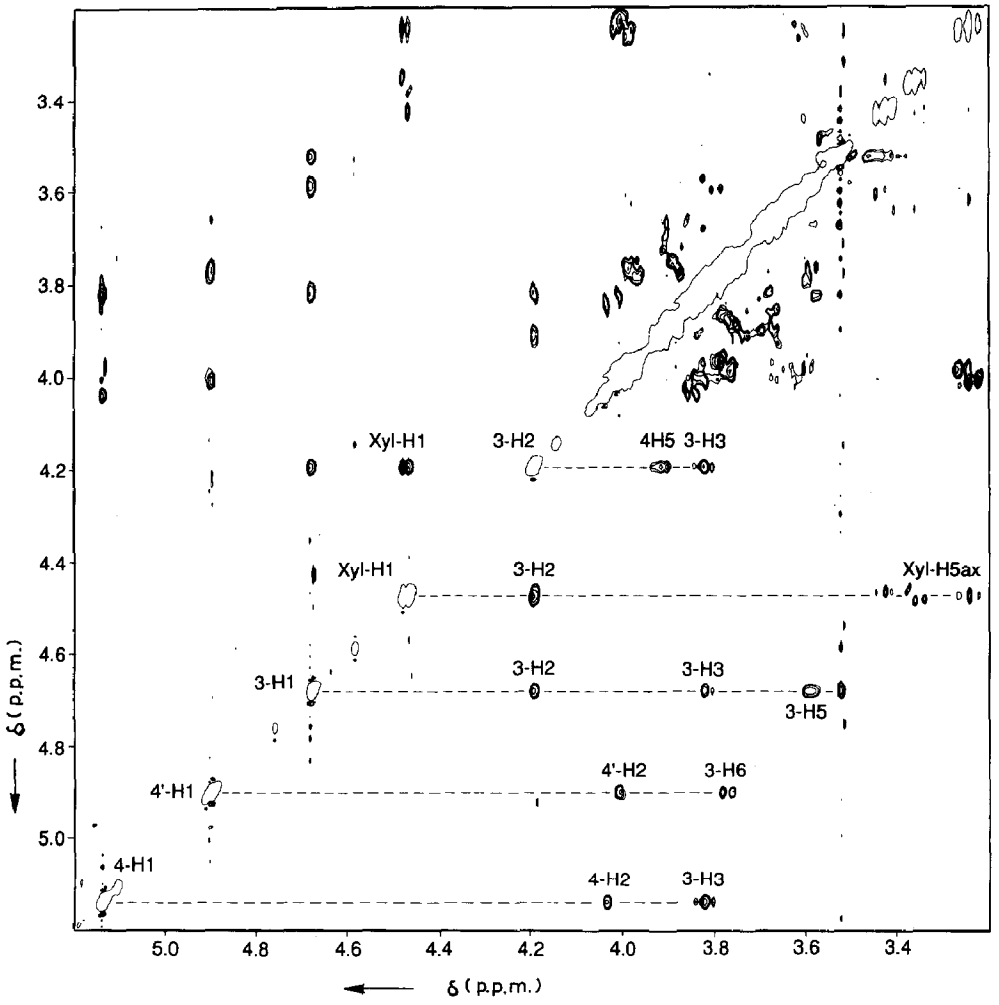

Fig. 1. 500-MHz ^1H–^1H ROESY spectrum of β-D-Xyl-(1→2)-[α-D-Man-(1→3)]-[α-D-Man-(1→6)]-β-D-Man-OMe (**3**). Lines are drawn to show scalar coupled networks. **3**-H2 means H-2 of Man-*3*.

between H-1 of Xyl and H-2 of Man-*3* points to a distance of 2.3 Å between these protons (Table I). Taking together the HSEA calculations and the distance constraint, the β-(1→2) linkage is determined at Φ/Ψ −70/120 (Table II). The iso-energy contours are not changed substantially by the attachment of α-D-Man in (1→6) linkage to Man-*3*, as is clear from a comparison of the HSEA calculations for this glycosidic linkage in β-D-Xyl-(1→2)-β-D-Man-OMe and **1** (data not shown).

β-D-Xyl-(1→2)-[α-D-Man-(1→3)]-β-D-Man-OMe (**2**). — For the α-Man-(1→3)-Man linkage, ROESY effects between H-1 of Man-*4* and H-3 of Man-*3*, and between H-5 of Man-*4* and H-2 of Man-*3*, show the H-1–H-3 and H-5–H-2 distances to be 2.3 and 2.4 Å, respectively (Table I). A combination of the Φ/Ψ ranges, as indicated by the two distance constraints, limits the orientation around the glycosidic linkage to

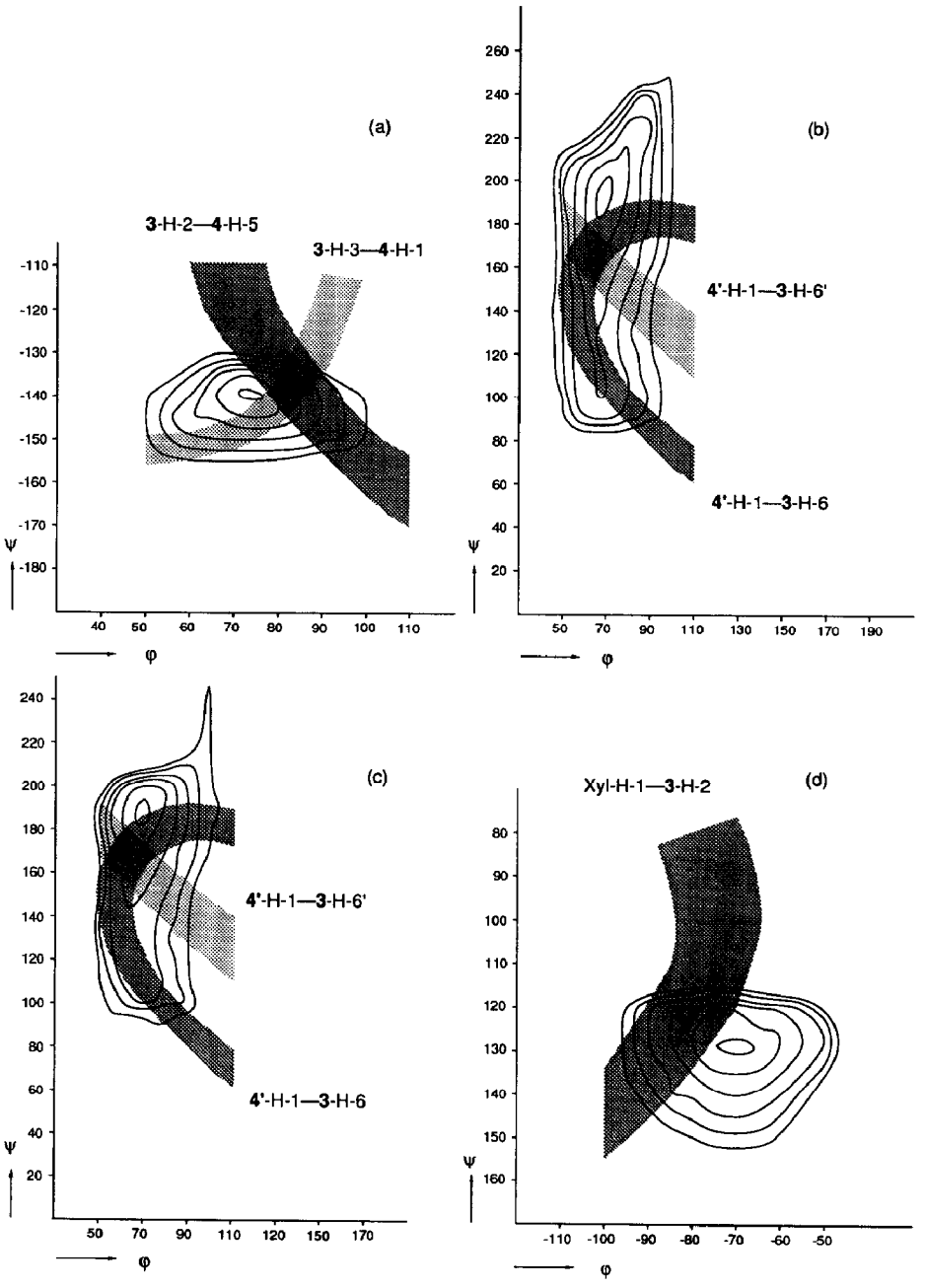

Fig. 2. Contour maps of the α-Man-(1→3)-Man linkage (a), the α-Man-(1→6)-Man linkage for the $P_{\omega=180}$ (b) and the $P_{\omega=60}$ (c) rotamer, and the β-Xyl-(1→2)-Man linkage (d) of **3**, showing iso-energy contours and marked areas with all Φ/Ψ combinations as indicated by the experimentally obtained distance constraints, allowing a deviation of twice the estimated error.

Φ/Ψ 80/−140 (Table II). For the β-Xyl-(1→2)-Man linkage, a distance constraint of 2.2 Å, as indicated by a ROESY effect between H-1 of Xyl and H-2 of Man-*3*, together with the results of the HSEA calculations, determine the conformation to be Φ/Ψ −80/125. A comparison of the calculations for this glycosidic linkage in β-D-Xyl-(1→2)-β-D-Man-OMe and **2** shows that the potential energy well is narrowed by Man-*4*, but not shifted to other regions (data not shown).

TABLE II

Torsional angles (Φ,Ψ) for the glycosidic linkages of **1**, **2**, and **3** as determined by ^{1}H–^{1}H ROESY measurements in combination with HSEA calculations

Linkage	Φ/Ψ	ω $P_{\omega=60}$:$P_{\omega=180}$
β-D-Xyl-(1→2)-[α-D-Man-(1→6)]-β-D-Man-OMe (**1**)		
α-Man-(1→6)-Man linkage	170/180	40:60
β-Xyl-(1→2)-Man linkage	−70/120	
β-D-Xyl-(1→2)-[α-D-Man-(1→3)]-β-D-Man-OMe (**2**)		
α-Man-(1→3)-Man linkage	80/−140	
β-Xyl-(1→2)-Man linkage	−80/125	
β-D-Xyl-(1→2)-[α-D-Man-(1→3)][α-D-Man-(1→6)]-β-D-Man-OMe (**3**)		
α-Man-(1→3)-Man linkage	80/−140	
α-Man-(1→6)-Man linkage	80/170	40:60
β-Xyl-(1→2)-Man linkage	−80/125	

β-D-Xyl-(1→2)-[α-D-Man-(1→3)]-[α-D-Man-(1→6)]-β-D-Man-OMe (**3**). — For the α-Man-(1→3)-Man linkage, interglycosidic ROESY effects between H-1 of Man-*4* and H-3 of Man-*3* and between H-5 of Man-*4* and H-2 of Man-*3* show the H-1–H-3 and the H-5–H-2 distances to be 2.3 and 2.4 Å, respectively (Table I). The Φ/Ψ areas, indicated by these distance constraints, are marked in the iso-energy contour map in Fig. 2a. The conformation of the (1→3) linkage, as defined by the cross-section of both areas, is identical to that of this linkage in **2** (Φ/Ψ 80/−140). For the α-Man-(1→6)-Man linkage, the rotamer population, as calculated from the vicinal coupling constants[8] $J_{5,6}$ (2.2 Hz) and $J_{5,6'}$ (5.3 Hz), is determined to be $P_{\omega=60}$:$P_{\omega=180}$: $P_{\omega=-60}$ = 40:60:0. Distance constraints between H-1 of Man-*4'* and H-6,6' of Man-*3* of 3.2 Å and 2.4 Å, respectively (Table I), determine the conformation at Φ/Ψ 80/170, in accordance with the HSEA calculations (Fig. 2b,c). For the β-Xyl-(1→2)-Man linkage, an interglycosidic ROESY effect between H-1 of Xyl and H-2 of Man-*3* points to a distance of 2.2 Å for this proton pair (Table I). In combination with the HSEA calculations, the conformation of the (1→2) linkage is described by Φ/Ψ −80/125 (Fig. 2d).

On the basis of the conformational data, molecular models of the trisaccharide and the tetrasaccharide in solution were constructed and are shown in Fig. 3, although it

should be kept in mind that these conformations reflect time-averaged structures. The torsional angles in the trisaccharides appear to be similar to the corresponding angles in the tetrasaccharide. The Φ/Ψ data for the (1→6) and (1→3) linkage in **1**, **2**, and **3** agree with those of an asialo diantennary structure[25,26] and the Φ/Ψ data for the (1→6) and (1→2) linkage in **1** and **3** agree with those in the carbohydrate chain of bromelain[9]. It is known[27] that the rotamer population about the C-5–C-6-linkage of Man-*3* can be influenced by adding a residue to the primary sequence. This influence was studied for several compounds. Comparison of the data for **1** and **3** reveals that the addition to **1** of Man-*4*, in α-(1→3) linkage to Man-*3*, does not affect the rotamer population about the C-5–C-6-linkage of Man-*3*. A comparison of the rotamer populations for **3** and for α-D-Man-(1→6)-[α-D-Man-(1→3)]-β-D-Man-(1→4)-β-D-GlcNAc-(1→4)-β-D-GlcNAc-OH[27,28] shows that Xyl, β-(1→2)-linked to Man-*3*, does not change the rotamer population about the C-5–C-6 bond of Man-*3* either. Finally, a comparison of the rotamer population about the C-5–C-6 bond of Man-*3* in **1** ($P_{\omega=60}$:$P_{\omega=180}$:$P_{\omega=-60}$ = 40:60:0) and in bromelain[9], α-D-Man-(1→6)-[β-D-Xyl-(1→2)]-β-D-Man-(1→4)-β-D-GlcNAc-(1→4)-[α-L-Fuc-(1→3)]-β-D-GlcNAc-(1→N)-Asn~ ($P_{\omega=60}$ >98%), establishes that the structural element β-D-GlcNAc-(1→4)-[α-L-Fuc-(1→3)]-β-D-GlcNAc-(1→N)-Asn~ does have an effect and induces the $P_{\omega=60}$ rotamer.

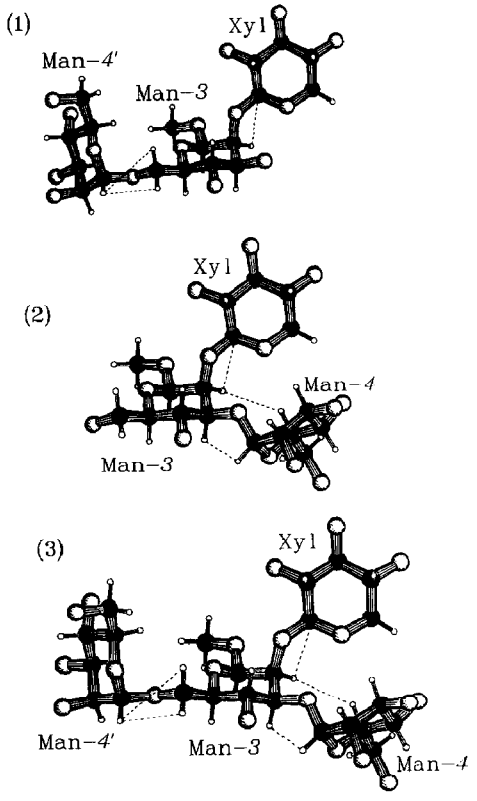

Fig. 3. Molecular models of **1**, **2**, and **3** as deduced from the ^1H–^1H ROESY and HSEA data (only the $P_{\omega=180}$ conformations are shown).

Taking into account the foregoing results, it can be found that the effects of changes in the primary structure of oligosaccharide chains on the time-averaged conformation are not easily predictable. Significant conformational changes will occur only if the additional residues have or induce attractive or repulsive interactions with other parts of the molecule. Therefore, measurements of n.O.e. effects, giving information about time-averaged short ^1H–^1H distances, in combination with energy calculations that afford the magnitude of the interactions, are of great importance for structural analysis. The ROESY experiment, provided it has been set up carefully, is a useful tool in conformational studies.

ACKNOWLEDGMENTS

This investigation was supported by the Netherlands Foundation for Chemical Research (SON) with financial aid from the Netherlands Organization for Scientific Research (NWO).

REFERENCES

1 J. A. van Kuik, R. A. Hoffmann, J. H. G. M. Mutsaers, H. van Halbeek, J. P. Kamerling, and J. F. G. Vliegenthart, *Glycoconj. J.*, 3 (1986) 27–34.
2 A. Sturm, J. A. van Kuik, J. F. G. Vliegenthart, and M. J. Chrispeels, *J. Biol. Chem.*, 262 (1987) 13 392–13 403.
3 G. D'Andrea, J. B. Bouwstra, J. P. Kamerling, and J. F. G. Vliegenthart, *Glycoconj. J.*, 5 (1988) 151–157.
4 J. A. van Kuik, H. van Halbeek, J. P. Kamerling, and J. F. G. Vliegenthart, *J. Biol. Chem.*, 260 (1985) 13 984–13 988.
5 J. A. van Kuik, R. P. Sijbesma, J. P. Kamerling, J. F. G. Vliegenthart, and E. J. Wood, *Eur. J. Biochem.*, 160 (1986) 621–625.
6 J. A. van Kuik, R. P. Sijbesma, J. P. Kamerling, J. F. G. Vliegenthart, and E. J. Wood, *Eur. J. Biochem.*, 169 (1987) 399–411.
7 J. Kerékgyártó, J. P. Kamerling, J. B. Bouwstra, J. F. G. Vliegenthart, and A. Lipták, *Carbohydr. Res.*, 186 (1989) 51–62.
8 J. B. Bouwstra, J. Kerékgyártó, J. P. Kamerling, and J. F. G. Vliegenthart, *Carbohydr. Res.*, 186 (1989) 39–49.
9 J. B. Bouwstra, E. C. Spoelstra, P. de Waard, B. R. Leeflang, J. P. Kamerling, and J. F. G. Vliegenthart, *Eur. J. Biochem.*, 190 (1990) 113–122.
10 A. A. Bothner-By, R. L. Stephens, and J.-M. Lee, *J. Am. Chem. Soc.*, 106 (1984) 811–813.
11 L. Braunschweiler and R. R. Ernst, *J. Magn. Reson.*, 53 (1983) 521–529.
12 A. Bax and D. G. Davis, *J. Magn, Reson.*, 63 (1985) 207–213.
13 A. Neuhaus, and J. Keeler, *J. Magn. Reson.*, 68 (1986) 568–574.
14 B. T. Farmer, II, and L. R. Brown, *J. Magn. Reson.*, 72 (1987) 197–202.
15 J. Breg, D. Romijn, J. F. G. Vliegenthart, G. Strecker, and J. Montreuil, *Carbohydr. Res.*, 183 (1988) 19–34.
16 K. Bock, *Pure Appl. Chem.*, 55 (1983) 605–622.
17 A. I. Kitaygorodsky, *Tetrahedron*, 14 (1961) 230–236.
18 C. M. Venkatachalam and G. N. Ramachandran, in G. N. Ramachandran (Ed.), *Conformation of Biopolymers*, Vol. 1, Academic Press, New York, 1967, p. 83.
19 H. Thøgersen, R. U. Lemieux, K. Bock, and B. Meyer, *Can. J. Chem.*, 60 (1982) 44–57.
20 D. Marion and K. Wüthrich, *Biochem. Biophys. Res. Commun.*, 117 (1983) 967–974.
21 B. Sheldrick and D. Akrigg, *Acta Crystallogr., Sect. B*, 36 (1980) 1615–1621.
22 A. Kumar, G. Wagner, R. R. Ernst, and K. Wüthrich, *J. Am. Chem. Soc.*, 103 (1981) 1354–1358.
23 A. L. Spek, in D. Sayre (Ed.), *Computational Crystallography*, Clarendon Press, Oxford, 1982, p. 528.
24 G. P. Wu, A. S. Serianni, and R. Barker, *J. Org. Chem.*, 48 (1983) 1750–1757.

25 J.-R. Brisson and J. P. Carver, *Biochemistry*, 22 (1983) 3680–3686.
26 O. Jardetzky, *Biochim. Biophys. Acta*, 621 (1980) 227–232.
27 S. W. Homans, R. A. Dwek, and T. W. Rademacher, *Biochemistry*, 26 (1987) 6571–6578.
28 S. W. Homans, R. A. Dwek, J. Boyd, M. Mahmoudian, W. G. Richards, and T. W. Rademacher, *Biochemistry*, 25 (1986) 6342–6350.